Propagation of optical vortex solitons due to the Gouy phase in strongly nonlocal nonlinear media*

Wu Xiao-Fei(吴晓飞), Deng Dong-Mei(邓冬梅), and Guo Qi(郭 旗)†

Key Laboratory of Photonic Information Technology of Guangdong Higher Educaiton Institutes, South China Normal University, Guangzhou 510631, *China*

(Received 29 December 2010; revised manuscript received 12 March 2011)

In this paper, we present a study on the propagation of the symmetrical optical vortices formed by two collinear Laguerre–Gauss solitons in strongly nonlocal nonlinear media. The optical vortices, which move along the beam axis as the light propagates, result in a rotation of the beam's transverse profile. This physical reason of the rotation is the Gouy phase acquired by the component beams.

Keywords: optical vortices, Gouy phase, strongly nonlocal nonlinear media

PACS: 42.25.Bs, 42.65.–K, 42.65.Tg **DOI:** 10.1088/1674-1056/20/8/084201

1. Introduction

Optical spatial solitons have been extensively studied in nonlocal nonlinear media.[1−28] The evolution of the optical beams in the nonlocal nonlinear media satisfies the nonlocal nonlinear Schrödinger equation (NNLSE).[1−3] In 1997, Snyder and Mitchell simplified the NNLSE to the Snyder–Mitchell model[18] in the case of strong nonlocality. In 2004, by using the Taylor expansion method,[3−5] Guo's group obtained a new approximate model for the NNLSE in the strongly nonlocal nonlinear media (SNNM) with the symmetrical real spatial response function. The exact analytical Laguerre–Gauss (LG) solutions of the NNLSE have already been derived in SNNM in a cylindrical coordinate system for the case of strong nonlocality.[6,7]

In recent years, the propagation of optical vortices has attracted much attention.[21−42] Optical vortices, which are associated with the phase singularity, are one of the most interesting and fundamental optical singularities exhibited by wave fields. Optical vortices are surrounded by a wave field whose phase advances around the vortex, and whose associated wavefront carries orbital angular momentum.[30,33] However, the propagation dynamics of the symmetrical optical vortex solitons obtained by two collinear superpositions of LG ring vortex solitons has not been studied in SNNM.

In this paper, we study the dynamical propagation of the symmetrical optical vortices formed by two collinear superpositions of LG ring vortex solitons. We find that in these composite solitons, the optical vortices appear, and upon propagation these composite solitons move along the beam axis with a periodic rotation of the soliton profile. The motion of these optical vortices can be well interpreted by the Gouy phase.

This paper develops its structure as follows. In Section 2, we briefly show the LG modes of the simplified model for the NNLSE and the composite vortices. In Section 3, we discuss two cases of composite solitons that are obtained when two collinear LG solitons interact and we discuss the effect of parameters. In Section 4, we also discuss the propagation of these solitons and their connection to the Gouy phase. A conclusion is given in Section 5.

2. LG modes of the simplified model for the NNLSE and composite vortices

2.1. LG modes of the simplified model for the NNLSE

The propagation of the $(1+2)$-dimensional optical beams in nonlocal nonlinear media is modeled by

*Project supported by the National Natural Science Foundation of China (Grant Nos. 10904041 and 10674050), the Specialized Research Fund for the Doctoral Program of Higher Education of China (Grant No. 20094407110008), and the Specialized Research Fund for Growing Seedlings of the Higher Education of Guangdong Province, China (Grant No. C10087).

†Corresponding author. E-mail: guoq@scnu.edu.cn

© 2011 Chinese Physical Society and IOP Publishing Ltd

the NNLSE

$$\mathrm{i}\frac{\partial\psi}{\partial z}+\mu\Delta_{\perp}\psi+k\frac{\Delta n}{n_0}\psi=0, \tag{1}$$

where $\psi=\psi(\boldsymbol{r},z)$ is a paraxial beam, z is the longitudinal coordinate, $\mu=1/2k$, $k=\omega n_0/c$ is the wavenumber in the media without nonlinearity, n_0 is the linear refractive index of the media, $\Delta_{\perp}$ is the two-dimensional transverse Laplacian operator, $\Delta n=n_2\int R(\boldsymbol{r}-\boldsymbol{r}')|\phi(\boldsymbol{r}',z)|^2\mathrm{d}^2\boldsymbol{r}'$ is the nonlinear index coefficient, $\boldsymbol{r}$ and $\boldsymbol{r}'$ are the two-dimensional transverse coordinate vectors and R is the normalized symmetrical real spatial response function of the media.

For the strongly nonlocal case, the NNLSE can be deduced as the Snyder–Mitchell linear model, which can be written in the form in cylindrical coordinates (r,φ,z),[1,5−7]

$$\mathrm{i}\frac{\partial\psi}{\partial z}+\frac{\mu}{r}\frac{\partial\psi}{\partial r}+\mu\frac{\partial^2\psi}{\partial r^2}+\frac{\mu}{r^2}\frac{\partial^2\psi}{\partial\varphi^2}-\frac{n_2}{2n_0}k\gamma P_0r^2\psi=0, \tag{2}$$

where $r=|\boldsymbol{r}|$ is the radial coordinate, γ is the material parameter associated with the response function $R(r)$ and P_0 is the input power at $z=0$.

In SNNM, when $P_0=P_{\mathrm{c}}$, diffraction is exactly balanced by nonlinearity and these are LG solitons which preserve their widths as they propagate in the straight path along the z axis. The expressions of LG solitons can be written as[6,7]

$$\psi_{pm}=\frac{C_{pm}}{w_0}\left(\frac{r}{w_0}\right)^{|m|}L_p^m\left(\frac{r^2}{w_0^2}\right)\mathrm{e}^{-r^2/2w_0^2}\,\mathrm{e}^{\mathrm{i}(m\varphi-\phi)}, \tag{3}$$

where w_0 is the beam radius of LG solitons, $\phi=(2p+|m|+1)z/z_{\mathrm{R}}$ is the Gouy phase, which is different from that in linear media,[30,38,39] and $z_{\mathrm{R}}=kw_0^2$ is the Rayleigh range.

2.2. Composite vortices

The vortex LG solitons can be obtained as $m\neq0$. A general LG soliton mode has p radial nodes in its amplitude. In this paper, we limit ourselves to the LG solitons with single-ringed modes with $p=0$, equation (3) is simplified to the $(0m)$-mode LG solitons

$$\psi_{0m}=\left(\frac{1}{\pi|m|!}\right)^{1/2}\frac{1}{w_0}\left(\frac{r}{w_0}\right)^{|m|}\mathrm{e}^{-r^2/2w_0^2}\,\mathrm{e}^{\mathrm{i}(m\phi-\varphi)}. \tag{4}$$

Equation (4) represents a family of the LG solitons that have a distinct intensity profile consisting of a bright vortex ring. It is a phase vortex of topological charge m at the centre of the bright ring. The radius of the bright ring is the distance from the centre to the point where the intensity is maximum, which can be obtained from

$$\rho=\sqrt{|m|}w_0. \tag{5}$$

Obviously, the radius of the bright ring of the intensity distribution of the $(0m)$-mode LG solitons increases when $|m|$ increases.

To discuss the general optical vortices, extending the linear analysis[30,33] to the nonlinear case, we consider superposing two collinear LG solitons with topological charges m_1 and m_2. The total amplitude of the composite soliton can be written as

$$\psi_{\mathrm{T}}=\sin\theta\psi_{m_1}+\cos\theta\psi_{m_2}\,\mathrm{e}^{\mathrm{i}\delta}, \tag{6}$$

where δ is the relative phase between the two component solitons. The ratio of the amplitudes of the two LG solitons is given by

$$\alpha=\sqrt{\frac{I_1}{I_2}}=\tan\theta, \tag{7}$$

where I_1 and I_2 are the intensities of the two LG solitons. In the following we will discuss two cases of the composite soliton generated in this way.

3. Two cases and the effect of parameters

3.1. Case $|m_1|<|m_2|$

When $|m_1|<|m_2|$, the structure of the resulting composite soliton is a vortex of charge m_1 in the centre of the soliton surrounded by $|m_1-m_2|$ single-charged peripheral vortices of sign $\sigma_2=m_2/|m_2|$. These peripheral vortices are located at the same radial distance r_{v} and distributed at different angles ϕ_{v}, which are given by

$$r_{\mathrm{v}}=w_0\left(\frac{|m_2|!}{|m_1|!}\alpha^2\right)^{1/2(|m_2|-|m_1|)}, \tag{8}$$

$$\phi_{\mathrm{v}}=\frac{\delta+n\pi}{m_2-m_1}, \tag{9}$$

where $n=1,\ldots,(2|m_1-m_2|-1)$ is an odd integer for each of the peripheral vortices. It is easy to find from Eq. (5) that the intensity radii of the two LG soliton modes are different, which leads to these peripheral vortices. That is to say, the shear in the phase of the two LG soliton modes located at different radii creates the peripheral vortices. In order to understand this easily, we can consider that when the amplitude

of the component solitons are the same, i.e. $\alpha = 1$. The region of $r < r_{\rm v}$ is dominated by the soliton with smaller topological charge $|m_1|$, and the region of the $r > r_{\rm v}$ is dominated by the soliton with larger topological charge $|m_2|$. The peripheral vortices are located precisely at $r = r_{\rm v}$.

The angles $\phi_{\rm v}$, where the vortices are located, are phases of the dominant modes $m_1\phi$ and $m_2\phi$ on each side of the boundary, which differ by an odd multiple of 1/4. Actually, equation (9) can be obtained from $m_2\phi - m_1\phi - \delta = n\pi$. When the relative phase δ is changed, the peripheral vortices rotate an angle about the centre of the beam consistent with the change of their angular position.

In Fig. 1, the first and second rows show patterns of the resulting composite solitons corresponding to $m_1 = -1$ and $m_2 = +4$. The top row shows the resulting composite soliton for several values of $\theta = \tan^{-1}\alpha$ in increments of $\pi/8$ with $\delta = 0$. The left-most pattern, corresponding to the case $\theta = 0$, consists of a purely $m_2 = +4$; the right-most one corresponds to the case $\theta = \pi/2$, where the beam is purely the $m_1 = -1$ component. The middle pattern corresponds to the case $\theta = \pi/4$, where we can clearly see a vortex with charge -1 in the centre of the beam, and five optical vortices of charge $+1$ distributed symmetrically in the periphery. In a cycle, the peripheral vortices move outwards as θ is increased.

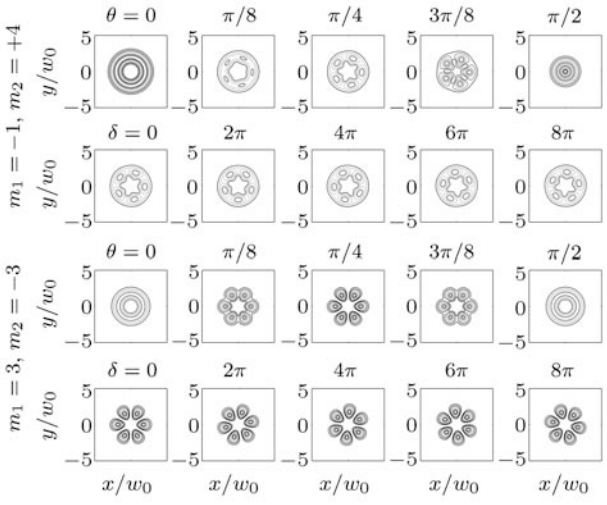


Fig. 1. Patterns of the composite solitons at $z = 0$. Top row: the composite soliton as a function of the relative amplitude α for $m_1 = -1$ and $m_2 = 4$, where α is determined by the θ via $\alpha = \tan\theta$, and $\delta = 0$. The second row: the composite soliton as a function of the relative phase δ for $m_1 = -1$ and $m_2 = 4$, and $\alpha = 1$. The third row: the composite soliton as a function of α for $m_1 = +3$ and $m_2 = -3$, and $\delta = 0$. The fourth row: the composite soliton as a function of δ for $m_1 = +3$ and $m_2 = -3$, and $\alpha = 1$.

The second row shows the resulting composite soliton as δ is changed while $\alpha = 1$. From Eq. (9), if we change δ by $\Delta\delta$, the pattern will rotate by $\Delta\phi_{\rm v} = \Delta\delta/(m_2 - m_1)$. A change in phase $\Delta\delta = 2\pi$ corresponding to a rotation of the composite soliton is $2\pi/5$.

3.2. Case $|m_1| = |m_2|$

In this case, there are no peripheral vortices in the composite soliton for any relevant parameters. When $\alpha \neq 1$, the phase at the nodes varies continuously. When the amplitudes of the component solitons are the same: $\alpha = 1$, $2|m_1|$ angular nodes are symmetrically distributed at angles $\phi_{\rm v}$ about the beam axis. At the nodes, the phase abruptly switches by π.

In Fig. 1, the third and fourth rows show the resulting composite solitons corresponding to $m_1 = +3$ and $m_2 = -3$. In the third row, θ is changed in increments of $\pi/8$ while keeping a fixed value of $\delta = 0$. The left-most and right-most patterns are the solitons with $m_2 = -3$ and $m_1 = +3$, respectively. In the middle, both component solitons have equal amplitude. We can see the π difference between adjacent lobes by the discontinuous shift in the fringes from lobe to lobe. The fourth row shows the component solitons taken for different values in δ increments of 2π for $\alpha = 1$. A change in phase $\Delta\delta = 2\pi$ corresponding to a rotation of the composite soliton is $2\pi/5$.

4. Propagation dynamics of optical vortices due to Gouy phase

The symmetrical optical vortices rotate about the beam axis as the composite solitons propagate. This is because the Gouy phase of the component solitons is different. The Gouy phase for LG solitons with topological charge m and radial mode p is given by

$$\varphi = (2p + |m| + 1)z/z_{\rm R}, \tag{10}$$

where $z_{\rm R}$ is the Rayleigh range.

Now letting $p = 0$, we consider the Gouy phase of single-ringed component beams, the peripheral vortices are located at angles

$$\phi_{\rm v} = \phi_n + \phi_l = \frac{\delta + n\pi}{m_2 - m_1} + \frac{|m_2| - |m_1|}{m_2 - m_1}\frac{z}{z_{\rm R}}, \tag{11}$$

where

$$\phi_n = \frac{\delta + n\pi}{m_2 - m_1}, \quad \phi_l = \frac{|m_2| - |m_1|}{m_2 - m_1} z/z_{\rm R}.$$

By keeping the dynamic phase δ constant, the angular changes at the vortex position between two points along the beam propagation direction is

$$\Delta\phi_{\rm v} = \frac{|m_2| - |m_1|}{m_2 - m_1}\frac{z}{z_{\rm R}}. \tag{12}$$

According to the different values of m_1 and m_2 in Eq. (12), we can discuss three cases. The first case is $|m_1| \neq |m_2|$ and $\sigma_1 = -\sigma_2$, equation (12) changes into

$$\Delta\phi_{\rm v} = \sigma_2\frac{|m_2| - |m_1|}{|m_2| + |m_1|}\frac{z}{z_{\rm R}}. \tag{13}$$

In this case, when $m_1 = 0$, the maximum rotation of the beam is π when $z/z_{\rm R} = \pi$. The rotation speed will decrease when m_1 increases.

To confirm the correctness of the solutions, numerical simulation of Eq. (1) is carried out by applying the split-step Fourier method. We set Eq. (6) at $z = 0$ as the input function, and the material response is fixed to the Gaussian function, i.e., $R(r) = 1/(2\pi w_{\rm m}^2)\exp[-r^2/(2w_{\rm m}^2)]$, here $w_{\rm m}$ is the characteristic length of the material response. The parameter $\alpha = w_0'/w_{\rm m}$ is the degree of nonlocality, and w_0' is the second-order moment width of the input function.

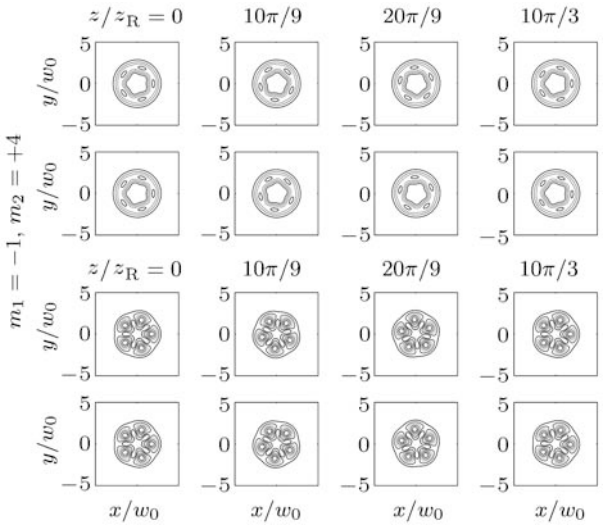


Fig. 2. Propagation dynamics of the composite solitons for $m_1 = -1$ and $m_2 = +4$. Top row: transverse normalized intensity distribution from the analytical solution, $\theta = \pi/8$ and $\delta = 0$. The third row: transverse normalized intensity distribution from the analytical solution, $\theta = 3\pi/8$ and $\delta = 0$. The second and fourth rows are the numerical simulation of the first and third rows, respectively. The degree of the nonlocality is 0.1.

Figure 2 shows propagation dynamics of the composite solitons created by the two collinear LG solitons with charge $m_1 = -1$ and $m_2 = +4$. Comparisons of the exact analytical solutions with numerical simulations of Eq. (1) show that the analytical solutions of Eq. (6) are in good agreement with the numerical simulations in the case of strong nonlocality. Letting $\Delta\phi_{\rm v} = 2\pi$, we can obtain a cycle of propagation of the composite solitons, and $z/z_{\rm R} = 10\pi/3$. It is clear that the vortices rotate as the composite soliton propagates along the z axis. However, the transverse normalized intensity distribution for $\theta = \pi/8$ is different from that for $3\pi/8$.

Figure 3 illustrates the propagation dynamics of composite solitons in one cycle, corresponding to $m_1 = -1$ and $m_2 = +4$. The parameters of the top row are chosen as $\theta = \pi/4$ and $\delta = 0$, and the third row $\theta = \pi/4$ and $\delta = 2\pi$. Compared with the leftmost figure of the first row and that of the third row, we can find obviously the locations of the vortices at $z = 0$ are distributed at different angles. This can be explained by different values of δ in Eq. (11), so the initial locations of each optical vortex is determined by $\phi_{\rm v}$.

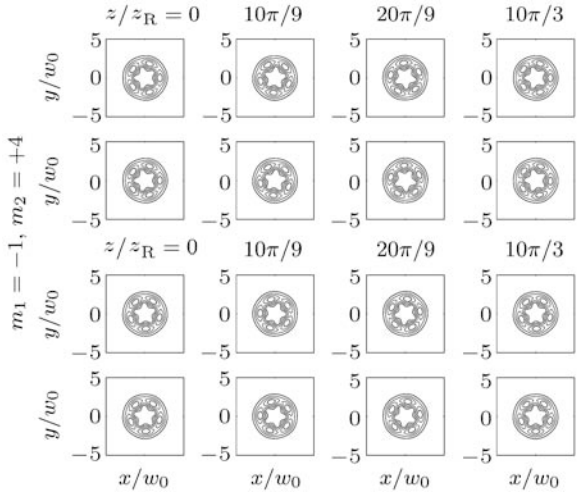


Fig. 3. Propagation dynamics of the composite solitons for $m_1 = -1$ and $m_2 = +4$. Top row: transverse normalized intensity distribution obtained from the analytical solution, $\theta = \pi/4$ and $\delta = 0$. The third row: transverse normalized intensity distribution obtained from the analytical solution, $\theta = \pi/4$ and $\delta = 2\pi$. The second and fourth rows are the numerical simulation of the first and third rows, respectively. The degree of the nonlocality is 0.1.

The second case is $|m_1| \neq |m_2|$ and $\sigma_1 = \sigma_2$. In this case we have

$$\Delta\phi_{\rm v} = \sigma_2\frac{z}{z_{\rm R}}, \tag{14}$$

the resulting composite solitons have two possible cases: symmetric and asymmetric cases, depending on the values of the topological charge of the component

solitons. Figure 4 shows the propagation dynamics of the composite soliton created by the superposition of two collinear LG solitons with charge $m_1 = +2$ and $m_2 = +4$.

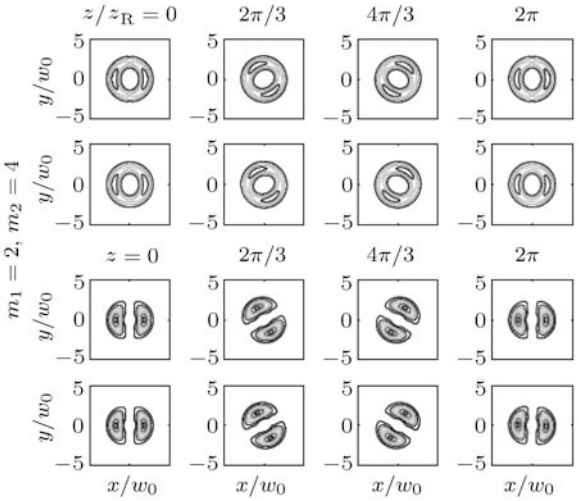


Fig. 4. Propagation dynamics of the composite solitons for $m_1 = +2$ and $m_2 = +4$. Top row: transverse normalized intensity distribution from the analytical solution, $\theta = \pi/8$ and $\delta = 0$. The third row: transverse normalized intensity distribution from the analytical solution, $\theta = 3\pi/8$ and $\delta = 0$. The second and fourth rows are the numerical simulations. The degree of the nonlocality is 0.1.

The third case is $|m_1| = |m_2|$ and $\sigma_1 = -\sigma_2$. In this case we have

$$\Delta\phi_v = 0. \tag{15}$$

This case is an exception to the general case: the composite soliton contains no peripheral vortices for fixed values of the relevant parameters as the composite soliton propagates along the z axis. Figure 5 shows propagation dynamics of the composite solitons created by the two collinear LG solitons with charge $m_1 = +3$ and $m_2 = -3$. In this case, the analytical solutions of Eq. (6) are also in good agreement with the numerical simulations of Eq. (1) in the case of strong nonlocality. Because the amplitudes of the component beams are equal, the resulting composite beams are the same for $\theta = \pi/8$ and $\theta = 3\pi/8$. In Fig. 6, we can observe the initial adjacent lobes of the composite beam which are distributed at different angles when the value of the parameter δ is different.

Comparison of the composite vortices in SNNM with those in the linear media,[30,38,39] it is easy to find that the propagation dynamics is different due to the different Gouy phases.

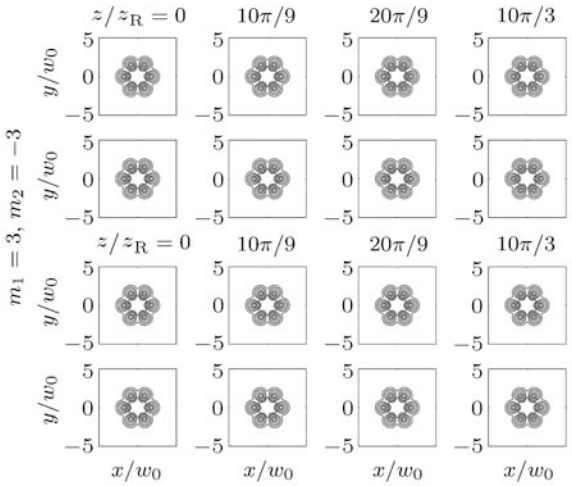


Fig. 5. Propagation dynamics of the composite solitons for $m_1 = +3$ and $m_2 = -3$. Top row: transverse normalized intensity distribution from the analytical solution, $\theta = \pi/8$ and $\delta = 0$. The third row: transverse normalized intensity distribution from the analytical solution, $\theta = 3\pi/8$ and $\delta = 0$. The second and fourth rows are the numerical simulations of the first and third rows, respectively. The degree of the nonlocality is 0.1.

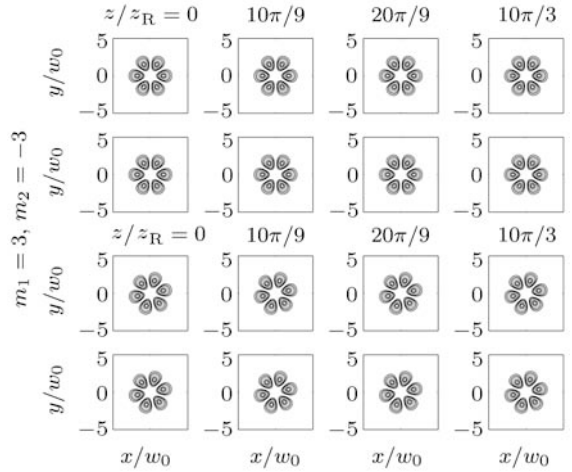


Fig. 6. Propagation dynamics of the composite solitons for $m_1 = +3$ and $m_2 = -3$. Top row: transverse normalized intensity distribution from the analytical solution, $\theta = \pi/4$ and $\delta = 0$. The third row: transverse normalized intensity distribution from the analytical solution, $\theta = \pi/4$ and $\delta = 2\pi$. The second and fourth rows are the numerical simulations of the first and third rows, respectively. The degree of the nonlocality is 0.1.

For the symmetric case, the vortices move along the z axis as the composite soliton propagates, resulting in a rotation of the beam's transverse profile. For the asymmetric case, the vortices also move along the z axis as the composite soliton propagates, resulting in a rotation of the beam's transverse profile, but the centre of the composite soliton is changing and deviating from the z axis continuously. Snyder–Mitchell linear model is valid for the symmetric case, but invalid for the asymmetric case.

5. Conclusion

In conclusion, the propagation of the symmetrical optical vortices formed by the superpositions of two collinear LG solitons in SNNM has been studied. The analytical results are in good agreement with the numerical simulations of NNLSE in the case of strong nonlocality. We find that the symmetrical optical vortices, which move along the beam axis as the light propagates, result in a periodic rotation of the beam's transverse profile. This rotation can be well explained by the Gouy phase acquired by the component solitons.

References

[1] Snyder A W and Mitchell D J 1997 *Science* **276** 1538

[2] Krolikowski W, Bang O, Nikolov N I, Neshev D, Wyller J, Rasmussen J J and Edmundson D 2004 *J. Opt.* B: *Quantum Semiclass. Opt.* **6** S288

[3] Guo Q, Luo B, Yi F, Chi S and Xie Y 2004 *Phys. Rev.* E **69** 016602

[4] Guo Q 2004 *Proc. SPIE* **5281** 581

[5] Xie Y and Guo Q 2004 *Opt. Quantum Electron.* **36** 1335

[6] Deng D M and Guo Q 2008 *J. Opt.* A: *Pure Appl. Opt.* **10** 035101

[7] Zhong W P 2008 *Phys. Rev.* A **78** 013826

[8] Deng D M, Zhao X, Guo Q and Lan S 2007 *J. Opt. Soc. Am.* B **24** 2537

[9] Skupin S, Saffman M and Królikowski W 2007 *Phys. Rev. Lett.* **98** 263902

[10] Kartashov Y V, Vysloukh V A and Torner L 2004 *Phys. Rev. Lett.* **93** 153903

[11] Buccoliero D, Desyatnikov A S, Krolikowski W and Kivshar Y S 2008 *Opt. Lett.* **33** 198

[12] Rotschild C, Schwartz T, Cohen O and Segev M 2008 *Nature Photonics* **2** 371

[13] Hu W, Zhang T, Guo Q, Xuan L and Lan S 2006 *Appl. Phys. Lett.* **89** 071111

[14] Conti C, Peccianti M and Assanto G 2003 *Phys. Rev. Lett.* **91** 073901

[15] Conti C, Peccianti M and Assanto G 2004 *Phys. Rev. Lett.* **92** 113902

[16] Peccianti M, Conti C and Assanto G 2004 *Nature* **432** 733

[17] Ouyang S G, Hu W and Guo Q 2007 *Phys. Rev.* A 2007 **76** 053832

[18] Shen Y R 1997 *Science* **276** 1520

[19] Kartashov Y V, Torner L, Vysloukh V A and Mihalache D 2006 *Opt. Lett.* **31** 1483

[20] Mihalache D, Mazilu D, Lederer F, Crasovan L C, Kartashov Y V, Torner L and Malomed B A 2006 *Phys. Rev.* E **74** 066614

[21] Mihalache D, Mazilu D, Lederer F, Malomed B A, Kartashov Y V, Crasovan L C and Torner L 2006 *Phys. Rev.* E **73** 025601

[22] He Y J, Malomed B A, Mihalache D and Wang H Z 2008 *Phys. Rev.* A 2008 **77** 043826

[23] He Y J, Malomed B A, Mihalache D and Wang H Z 2008 *Phys. Rev.* A **78** 023824

[24] Deng D M, Guo Q and Hu W 2009 *Opt. Lett.* **34** 43

[25] Deng D M and Guo Q 2008 *J. Phys.* B: *At. Mol. Opt. Phys.* **41** 145401

[26] Deng D M, Guo Q and Hu W 2008 *J. Phys.* B: *At. Mol. Opt. Phys.* **41** 225402

[27] Deng D M, Guo Q and Hu W 2009 *Phys. Rev.* A **79** 023803

[28] Deng D M and Guo Q 2010 *Opt. Commun.* **283** 3777

[29] Andrews D L 2008 *Structured Light and Its Applications: An Introduction to Phase-Structured Beams and Nanoscale Optical Forces* (Builington: Academic Press-Elsevier)

[30] Baumann S M, Kalb D M, MacMillan L H and Galvez E J 2009 *Opt. Express* **17** 9818

[31] Allen L, Beijersbergen M W, Spreeuw R J C and Woerdman J P 1992 *Phys. Rev.* A **92** 8185

[32] Indebetow G 1993 *J. Mod. Opt.* **40** 73

[33] Galvez E J, Smiley N and Fernandes N 2006 *Proc. SPIE* **6131** 19

[34] Galvez E J and Baumann S M 2008 *Proc. SPIE* **6905** 6905D-1

[35] Maleev I D and Swartzlander G A 2003 *J. Opt. Soc. Am.* B **20** 1169

[36] Kalb D M and Galvez E J 2009 *Proc. SPIE* **7227** 7227B-1

[37] Hamazaki J, Mineta Y, Oka K and Morita R 2006 *Opt. Express* **14** 8382

[38] Cheng K, Liu P S and Lü B D 2008 *Chin. Phys.* B 2008 **17** 1743

[39] Yan H W, Cheng K and Lü B D 2008 *Opt. Laser Tech.* **40** 967

[40] He D, Gao Z H, Lü B D and Yan H W Interaction of two Edge Dislocations in Free-Space Propagation, to be Published in Chinese Physics B.

[41] Li J L 2010 *Chin. Phys.* B **19** 104001

[42] Li J L 2010 *Chin. Phys.* B **19** 124001